PLANUM TEMPORALE: MORPHOLOGIC TAXONOMY OF THE POSTERIOR SUPERIOR TEMPORAL PLANE

By

Bryan Wong

Audiology Doctoral Project submitted to the faculty of the

DEPARTMENT OF SPEECH, LANGUAGE, AND HEARING SCIENCES

In Partial Fulfillment of the Requirements

For the Degree of

DOCTOR OF AUDIOLOGY

In the Graduate College

THE UNIVERSITY OF ARIZONA

2019

THE UNIVERSITY OF ARIZONA
GRADUATE COLLEGE

As members of the Audiology Doctoral Project Committee, we certify that we have read the Audiology Doctoral Project prepared by: Bryan Wong
titled: Planum Temporale: Morphological Taxonomy of the Posterior Superior Temporal Plane

and recommend that it be accepted as fulfilling the Audiology Doctoral Project requirement for the Degree of Doctor of Audiology.

F. E. Musiek — Date: 11/13/19
Frank Musiek, PhD

Barbara Cone — Date: 11/13/2019
Barbara Cone, PhD, CCC-A

Aneta Kielar — Date: 11/13/2019
Aneta Kielar, PhD

Andrew Fuglevand — Date: 11/13/2019
Andrew Fuglevand, PhD

Final approval and acceptance of this Audiology Doctoral Project is contingent upon the candidate's submission of the final copies of the Audiology Doctoral Project to the Graduate College.

I hereby certify that I have read this Audiology Doctoral Project prepared under my direction and recommend that it be accepted as fulfilling the Audiology Doctoral Project requirement.

F. E. Musiek — Date: 11/13/19
Frank Musiek, PhD
Dissertation Committee Chair
Speech, Language, and Hearing Sciences

Acknowledgements

I would like to express my sincere gratitude and special thanks to all my committee members; whose collective insights, knowledge, feedback, support and patience were instrumental in the completion of this project. I look up to all of you as leaders and role-models in your respective fields and hope to one day be at least half the scientists/researchers/professors that you all are. From the bottom of my heart, thank you.

I would also like to thank my parents, Michael and Robyn Wong, for their unending love and support in my academic journey.

Table of Contents

CONTENTS

List of Figures.....5

List of Tables.....5

Abstract.....6

Introduction.....8

- **Background**.....8
- **Motivation for Study**.....15

Methods.....17

- **Planum Temporale Boundaries**.....18
- **Heschl's Gyrus Variations**.....20
- **Posterior Sylvian Fissure Variations**.....21
- **Morphological Shape of Planum Temporale**.....21

Statistical Analyses.....22

Results.....23

Discussion.....29

- **Study Limitations and Future Goals**.....36

Conclusion.....38

References.....39

LIST OF FIGURES

FIGURE 1: *Example of procedure to obtain ROI* ……19

FIGURE 2: *Examples of Heschl's Gyrus variants*……..21

FIGURE 3: *Examples of PT morphological variants*……..24

FIGURE 4: *Bar graph (overall occurrence and mean surface area)* ……25

FIGURE 5: *Bar graph(occurrence and mean surface area by hemisphere)*…… 26

FIGURE 6: *Bar graph(occurrence and mean surface area by Sex)* ……27

LIST OF TABLES

TABLE 1: *Description of Planum Temporale in the literature*……16

TABLE 2: *Demographic variables of Study_group*……18

TABLE 3: *ANCOVA results summary*……30

TABLE 4: *Multiple Comparisons (Tukey HSD)*……30

Abstract

Background: Planum Temporale (PT) is a crucial neuroauditory structure located in the dorsal superior temporal plane (STP) posterior to Heschl's gyrus (HG). The PT has been implicated in complex auditory function and is well known for its preponderance of leftward asymmetry in normal brains and classic "*pie*- shaped" morphology. While a majority of cases have easily identifiable PT and HG, there exist some cases in which distinguishability of these two structures is difficult due to morphological variation. The goal of this study is to create a taxonomy of PT morphological features in order to improve the sometimes difficult identification and differentiation of PT from surrounding structures.

Methods: A total of 50 (100 hemispheres) healthy intact, high-resolution T1- weighted brain MRIs were obtained from Open Access Series of Imaging Studies (OASIS) and included in this retrospective study. There were 28 women and 22 men, all right-handed. Ages ranged from 18-57 (mean=26.44) years. A 3D cortical surface mesh (grey matter) for each brain was generated using FreeSurfer and manipulated to view the STP using BrainVISA Anatomist neuroimaging software. The PT was isolated from surrounding structures based on pre-defined anatomical criteria and subsequent surface area measurements, linear measurements and qualitative measures were made.

Results: A total of four PT configurations were identified: (1) Pie-shaped [45%], (2) Trapezoid-shaped [27%], (3) Rectangular-shaped [19%], and (4) None [9%]. Mean surface areas of measurable PT configurations were: 511.96 mm^2 for *"Pie-shaped*" (*n=45),* 517.36 mm^2 for "*Trapezoid-shaped*" (*n*=27*)* and 472.12mm^2 for "*Rectangular-shaped*" (*n=19)*. The fourth

category, "*None*" (*n*=9), was not calculable. There were significantly more *"Trapezoid-shaped"* PTs in females ($p<.05$*).* The "*None"* category occurred significantly more in males ($p<.05$*)* and in the right hemisphere ($p<.05$*).* Furthermore, the left hemisphere demonstrated significantly greater surface area for "*Pie-shaped"* PTs ($p<.05$).

Discussion/Conclusion: We believe that the proposed classifications is the first step in creating a comprehensive taxonomy of the STP. This will aid neuroanatomists, clinicians and students in terms of differentiation of sometimes complex topography of the STP.

Introduction

Background

The complex nature of the central auditory nervous system (CANS) has long been the target of research by hearing scientists, neurophysiologists and neuroanatomists. While some degree of processing auditory stimuli undoubtedly occurs along afferent subcortical auditory neural substrates, the auditory cortex is commonly believed to be the main computational hub that is responsible for integrating, synthesizing and deriving meaning from auditory stimuli. Cortical regions responsive to auditory stimuli are primarily located in the temporal lobe, more specifically, the superior temporal gyrus (STG) on the superior temporal plane (STP). Traditionally, the auditory cortex has been described as being composed of two parts: primary and secondary auditory areas. A cortical gray matter area called Heschl's gyrus (HG) is thought to make up a majority of the primary auditory area while neighboring grey matter regions, particularly posteriorly, are believed to mostly encompass secondary auditory areas (Hall et al., 2003; Hackett et al. 2001). A great deal of research describing the anatomy, physiology and function has been conducted on the primary auditory area encompassing HG, but relatively less is known about secondary auditory areas.

The Planum Temporale (PT) is a crucial neuroauditory grey matter structure that lies in the dorsal STP directly posterior to HG. The PT has been traditionally defined as a cortical secondary auditory area and has also been implicated in complex auditory processing abilities, including but not limited to: spectral-temporal processing, auditory working memory and auditory stream segregation (detailed below in *Function of PT*). However, researchers have barely begun to scratch the surface of the structure-function relationship even in a

neurologically normal population, and how differences could relate to neurologic pathologies that impact central auditory function.Part of the complication of determining this structure-function relationship lies within the ability to accurately identify these auditory neural substrates, namely HG and PT, on the superior temporal plane. While a majority of brains have easily identifiable HG and PT, there exist some cases in which the distinguishability of these two structures is difficult due to a high-degree of individual morphological variation. This is further complicated by differences in criteria that define the anatomical boundaries of PT. The purpose of this introduction is to review how PT has been previously classified. Then, a novel method for describing PT that aids in more reliable identification will be proposed.

The PT has generally been classified in three different ways: *cytoarchitectonically (microscopic), functionally* or by *gross morphology (macroscopic).* While a majority of previous research has described PT by the first two dimensions, *cytoarchitectonically* and *functionally*, there are still advances to be made in describing its gross morphology. The approach used in this paper aims to provide more detailed qualitative and quantitative descriptions by utilizing advanced 3D cortical reconstructions from each subjects' MRIs.

Cytoarchitecture of Planum Temporale

The area that would later be termed "planum temporale" was first described cytoarchitectonically in the early 20th century by illustrious German anatomist and neurologist Korbinian Brodmann. Using a Nissl method of cell staining, he divided post-mortem human brains into 52 segments based on distinct patterns of neuronal arrangement. Brodmann's area (BA) 41 denoted primary auditory cortex, or modern day HG, while the BA 42 and the posterior superior expanse of the BA 22 reflected auditory association cortex; later termed PT (Brodmann, 1909). In subsequent cytoarchitectonic maps, the neural substrate corresponding

to the PT area is also referred to as TA1 (von Economo and Koshinkas, 1925) and Tpt (Galaburda and Sanides, 1980). The cytoarchitecture of PT is demarcated by: wide columns of progressively larger pyramidal cells in Layer III that coalesce with granular cells in layer IV, a hypocellular Layer V with large cells compared to Layer VI, and radial striations projecting from layer III to layer VI (von Economo & Koshinkas, 1925; Galaburda & Sanides, 1980; Witelson et al. 1995). More recently, studies have examined the differences in microstructure between interhemispheric PTs. In a study using *in-vivo* neurite orientation dispersion and density imaging (NODDI) by Ocklenburg, Friedrich, Fraenz, et al. (2018), the left PT demonstrated both a greater density of axons and dendrites and overall more dendritic arborization compared to the right PT. This is consistent with human post-mortem studies which have also demonstrated a higher density of axons in the left PT and further described less overlap between the dendritic space of adjacent microcolumns (Seldon et al., 1981). The researchers of these studies suggest that this increased neuronal density in the left PT may predispose it to handle auditory temporal processing abilities which subserves speech processing.

However, there exists a degree of variability as to the expanse of this cytoarchitectonic pattern defining PT. Some studies have observed this area extruding onto the temporo-parietal convexity of the Sylvian Fissure opercula (Galaburda & Sanides, et al. 1978; Shapleske et al. 1999; Witelson et al., 1995) and others have observed it extending anteriorly to the posterior portion of HG duplications (Pfeifer et al., 1920; Von Economo & Horn, 1929; Penhune et al., 1996). As a result, differences in criteria describing the anatomical boundaries of PT based on these variable cytoarchitectonic studies have arisen. Given the observed cytoarchitectonic variation of the PT area, differentiation of PT from HG based solely on cytoarchitecture may not always be clear nor reliably generalizable.

Function of Planum Temporale

With the advent and continued advancement of imaging techniques, the relationship between *function* and the *cytoarchitecture* defining the PT area, described above, has been closely examined as a differentiating factor. The PT has been implicated in higher-order auditory processing including: auditory stream segregation, auditory working memory and spectral-temporal processes.

An fMRI study by Voulooumanos, Kiehl, Werker & Liddle (2001) investigated cortically active regions involved in auditory stream segregation in 15 healthy adults using an oddball detection task. Participants had to correctly differentiate between target speech, non-speech and tonal stimuli in the presence of a continual non-target 1000Hz tone. Overall, the authors observed that the left STG and PT were active, among other regions, across all stimulus types and that there was greater cortical activation when attending to the speech stimuli. Similarly, in a Positron Emission Tomography (PET) study by Zatorre, Evans, Meyer and Gjedde (1992), researchers demonstrated greater cerebral blood flow in primary auditory areas for white noise stimuli and distinctly greater cerebral blood flow in secondary auditory areas for speech consonant-vowel-consonant tokens. The authors of this paper contend that that the primary and secondary auditory areas are responsible for processing different components of complex auditory signals, but that they work in tandem for more holistic processing.

With regards to auditory working memory, an fMRI study by Papoutis, de Zwart, Jansma, et al. (2009) demonstrated increased bilateral activation of PT when subjects were instructed to mentally rehearse a four-syllable pseudo-word for six seconds before overtly or covertly repeating the pseudoword. In another fMRI by Koelsch, Schulze, Sammier, Fritz, Müller and Gruber (2009), the STG and PT were also observed to be bilaterally activated when

participants were presented with strings of four-syllables that were sung and then subsequently tasked with recalling either the tonal or verbal information of the stimuli.

In a Positron Emission Tomography (PET) study by Thivard, Belin, Zilbovicius, Poline, and Samson (2000) that examined cortically active regions in 8 right-handed males, researchers demonstrated greater activation of PT than HG with spectral motion of auditory stimuli compared to stationary stimuli. This finding is supported by subsequent fMRI and PET studies that also showed increased activation of PT bilaterally with spectral motion stimuli (Bremmer et al., 2001; Warren et al., 2002). Additionally, in another PET study examining 9 musically naive males, bilateral PTs were observed to be activated during duration and pitch pattern perception tasks that required an active response (Griffiths et al., 1999), similar to subsequent fMRI studies which utilized comparable paradigms (Binder et al., 2000; Hall et al., 2002).

The PT area is also observed to be implicated in dichotic listening. Hashimoto, Homae, Nakajima, et al. (2000) demonstrated greater activation of the posterior STP and PT when passive dichotic versus diotic speech stimuli were administered. In another interesting study that examined interhemispheric PT micro-structure and neurophysiologic processing of dichotically presented speech stimuli, Ocklenburg, Friedrich, Fraenz, et al. (2018) found that a higher density of dendrites and axons in the left hemisphere PT correlated with reduced N1 potential latency compared to the right hemisphere PT. The authors of this paper suggest that the overall increased synaptic connections found in the left PT predispose it for faster and more precise temporal processing that underlies perception of speech stimuli.

Given its location in the posterior recess of the Sylvian Fissure (SF), proximal to the temporo-parietal convexity, it is no surprise that PT has also been highly implicated in language processing. The left PT has been found to be active in language tasks such as: phonological retrieval, complex syntactic sequencing and semantic processing (Hickock et al., 2009; Obleser

& Kotz, 2009; Price et al., 2010, Deschamps & Tremblay, 2014). This is further corroborated by pathological studies which have demonstrated that lesions extending to the PT, particularly in the left hemisphere, manifest as written and spoken language comprehension deficits (Naeser et al., 1987; Dronkers et al., 2004; Kim & Paik, 2014) in conjunction to disrupting higher auditory processing such as spectro-temporal processing abilities (Shapleske et al., 1999).

One issue of solely depending on *functional* studies for differentiation between PT and HG is the overlap in activation between these auditory neural substrates and of other non-auditory areas. In all reviewed studies above, processing complex auditory stimuli typically triggers a network of cortically active brain regions and engages, at least partially, both PT and HG. Furthermore, pathological studies, mentioned previously, should be interpreted with caution as a majority of the included participants suffered cerebrovascular accidents whose lesions were diffuse and extended to other cortical areas. It is thus difficult to determine the degree of contribution and function of PT in speech processing based solely on lesion studies. Although imaging research has led to amazing insights into the auditory processing at the cortical level, it remains difficult to definitively isolate the true function of PT from HG due to some degree of overlap in activation and because anatomical differentiation has not been consistent.

Gross Morphology of Planum Temporale

Lastly, PT has previously been described by its macroscopic features including: surface area, cortical volume, linear dimensions, and symmetry between hemispheres. A preponderance for PT to be larger in the left compared to right hemisphere is prevalently described in the literature. In a classic study comparing the interhemispheric linear measurements of PT's lateral edge in 100 normal post-mortem human brains, Geschwind & Levitsky (1968) found that 65% of brains exhibited larger PTs in the left hemisphere, 11% of

brains had larger PTs in the right hemisphere and 24% of the brains exhibited relatively symmetrical PTs. Subsequent studies and findings observing this preponderance for left>right PT asymmetry in normal brains have not deviated from this initial study and has been replicated in other post-mortem studies (Galaburda et al., 1987; Teszner et al., 1972; Kopp et al., 1977; Falzi et al., 1982; Nikkuni et al., 1981). Additional post-mortem studies also replicated this left>right PT asymmetry in infants as well (Witelson & Pallie, 1973; Wada et al., 1975). In recent years, *in-vivo* surface area and volumetric studies made possible by 2D and 3D imaging techniques have also replicated this leftward asymmetry in normal intact brains (Foundas et al., 1994; Barta et al., 1995; Foundas et al., 1995; Steimetz & Galaburda, 1991; Kulynyc et al., 1993; St. George et al., 2017). Of more recent interest are studies examining pathologies related to abnormal PT asymmetry, which manifests either as an interhemispheric asymmetric reversal (Right>Left) or an interhemispheric symmetry between an individual's PTs. With regards to the former, cortical surface area/volume/thickness are observed to be abnormally larger in the right PT with slight reduction in the left PT. The latter describes instances in which the cortical surface area/volume/thickness is grossly normal for right PT but reduced in the corresponding left PT. Studies examining dyslexic populations have observed higher occurrences of both an abnormal reversal in PT right>left asymmetry (Hugdahl et al., 1998; Bloom et al., 2013; Altarelli et al., 2014) and abnormal interhemispheric symmetry between PTs (Larsen et al., 1990). Similarly, in imaging and post-mortem studies examining individuals with schizophrenia, higher occurrences of both abnormal reversals in PT right>left asymmetry (Barta et al., 1997; Falkai et al., 1997; Hasan et al., 2011) and abnormal interhemispheric symmetry (Kasai et al., 2003; Oertel-Knockel et al., 2013; Ratnanathar et al., 2013) between PTs have additionally been observed.

While quantitative measurements of these macroscopic features are important in studying normal and pathological populations, these studies do not necessarily aid in differentiation of auditory neural substrates on the STP. Delineation of PT from HG in these instances are based on *cytoarchitecture* and *functional* studies, and are thus subject to the same errors. Moreover, if two studies were to use differing PT boundary criteria, quantitative measures are subject to be under- or over-estimated. This is exemplified in a recent anatomical study by St. George et al. (2017) who examined 28 brain MRIs and demonstrated that surface area of PT was significantly smaller when cases of posterior HG duplication did not constitute part of the PT measurement and also when the posterior aspect of the SF extended superior-dorsally to a posterior ascending ramus (PAR). These results were replicated in a study by Tzourio-Mazoyer & Mazoyer (2017) which found similar influences of HG and SF variation on PT surface area.

Motivation for Study

While a majority of brains have easily identifiable Heschl's Gyri (HG) and PT, there exist some cases in which distinguishability of these two structures is difficult due to a high-degree of individual morphological variation. An example of this variation is apparent in Heschl's Gyrus, which morphologically manifests in various configurations and thus complicates accurate identification of the anterior border of PT. Since morphological variation is exhibited in HG, it is our hypothesis that there is also a degree of morphological variation in PT as well. Furthermore, PT has been described throughout the literature as manifesting only in a "*pie-shaped*" or "*triangular*" configuration (**see TABLE 1**). This could potentially lead to confusion and misidentification if PT has alternative morphological variants and researchers, students or clinicians rely on this anatomical landmark description. The primary goal of this study is to create a taxonomy of various PT morphological features in order to improve the sometimes

difficult identification and differentiation of PT and HG**.** Secondarily, the occurrence and surface areas of these various PT classifications will be evaluated with respect to hemisphere and gender. This study will address these specific questions to be answered: (a) What morphological variations of PT exist and how often do they occur overall and interhemispherically? (b) Do any of these PT morphological variations occur more often in a particular hemisphere or sex? (c) Are there surface area differences between these morphological variations?

Certain predictions have been made: (1) There will be other morphological variations of PT, but that the typical description of "*Pie-shaped*" will occur most frequently because it is the variation most commonly described in the literature (**see TABLE 1**); (2) It is predicted that new PT classifications will have larger surface areas in the left hemisphere compared to the right hemisphere similar to the previous studies showing leftward asymmetry; (3) PT classifications with more edges and vertices will comparatively have larger surface areas because it will widen the expanse of the measurable PT plane ; (4) There will be no significant sex differences in terms of PT variation occurrence but males will be exhibit overall greater PT surface area compared to females give a preponderance for male brains to be larger on average (Stein et al., 2012; Good et al., 2001; de Courten-Myers, 1999; Shapleske et al., 1999).

***TABLE 1: Description of Planum Temporale in the literature has been loosely described*.**

Authors	**PT Description**
Shapleske et al., 1995	*"…resembles an isosceles triangle…"*
Binder et al., 1996	*"…roughly a triangular shape…"*
Zach et al., 2009	*"…isosceles triangle…"*

Hikock & Saberi, 2012	*"…triangular surface on the supra-temporal plane…"*
Pahs et al., 2013	*"…triangular cortical surface…"*
Altarelli et al., 2014	*"This triangular structure…"*
Musiek & Baran, 2018	*"…wedge-shaped…"*

Methods

A total of 50 (100 hemispheres) healthy intact brain MRIs, 28 women and 22 men, were obtained sequentially from the Open Access Series of Imaging Studies (OASIS) and included in this retrospective study. Ages ranged from18-57 years, with a mean of 26.44 years, and all subjects were right-handed. High-resolution, T1- weighted magnetic resonance imaging (MRI) for each subject was obtained on a 7T Siemens Magnetom (Erlangen Germany) and also included MP-2RAGE T1 imaging (parameters: acquisition matrix 224 × 224 × 104, repetition time (TR) = 5000 ms, echo time (TE) = 2.62 ms, flip angle = 5 deg, field of view (FOV) = 224 mm, voxel size = 0.5 × 0.5 × 0.5 mm). The first 28 of these intact brain MRIs were used in a previous study by St. George et al. (2017). A 3D cortical surface mesh (grey matter) for each brain was then generated using FreeSurfer (Dale, Fischl, Serreno, 1999). Irrelevant structures, such as the skull, brainstem, eyes and white matter were extracted during this pre-processing stage. Additionally, normalization of intracranial volume to correct for cortical surface area variations between subjects was achieved by utilizing a verified automated atlas scaling technique (Buckener et al., 2004). Next, the BrainVISA Anatomist neuroimaging software (Le Troter, Auzias & Coulon, 2012), was used to manipulate 3D cortical meshes and view the Superior Temporal Plane. The frontal and parietal lobe were digitally excised using the knife-cut method to expose the STP (**see FIGURE 1a)**. The PT region-of-interest (ROI) was isolated using defined

boundary criteria **(see FIGURE 1b)** and then subsequently high-lighted for quantitative analysis. A custom PYTHON script was employed to obtain an overall surface area measurement of the region-of interest by summing the surface area of each comprising triangular unit of the mesh, for each individual brain. A separate neuroimaging software, *MANGO* (Lancaster & Martinez, 2016) was utilized to make linear measurement on previously defined PT ROIs.

TABLE 2: Demographic data for Study_group

	Study_Group
Mean(SD) Unless specified	***(N=50)***
Age	26.44(7.32)
Sex	22m/28f
Handedness *[n*= right handed (%)]	50 (100)
eTIV	1532447.70(15246.70)

Planum Temporale Boundaries

In order to delineate PT from its surrounding structures, certain criteria and clear boundaries were defined. In general terms, PT had to be a plane of cortical grey matter that was relatively level to its anterior HG. The *anterior border* was delimited by Heschl's transverse sulcus (Marie et al., 2015; Rademacher et al. 1993; St. George et al., 2017). In cases of duplicated HGs, the posterior most transverse sulcus was used. This is further corroborated by myeloarchitectonic studies that support this border differentiation of HG from PT (De Martino et al., 2015; Da Costa et al., 2011). The *medial* and *lateral* boundaries were demarcated by retro- insular white matter and the supero-lateral boundary of the Superior Temporal Gyrus, respectively (Shapleske et al., 1999; St. George et al., 2017). The *posterior* boundary was defined as the beginning of the Posterior Ascending Ramus (PAR), or the posterior termination of the main segment of the SF (Shapleske et al., 1999; St. George, 2017). These boundaries are exemplified in **FIGURE 1c**, below.

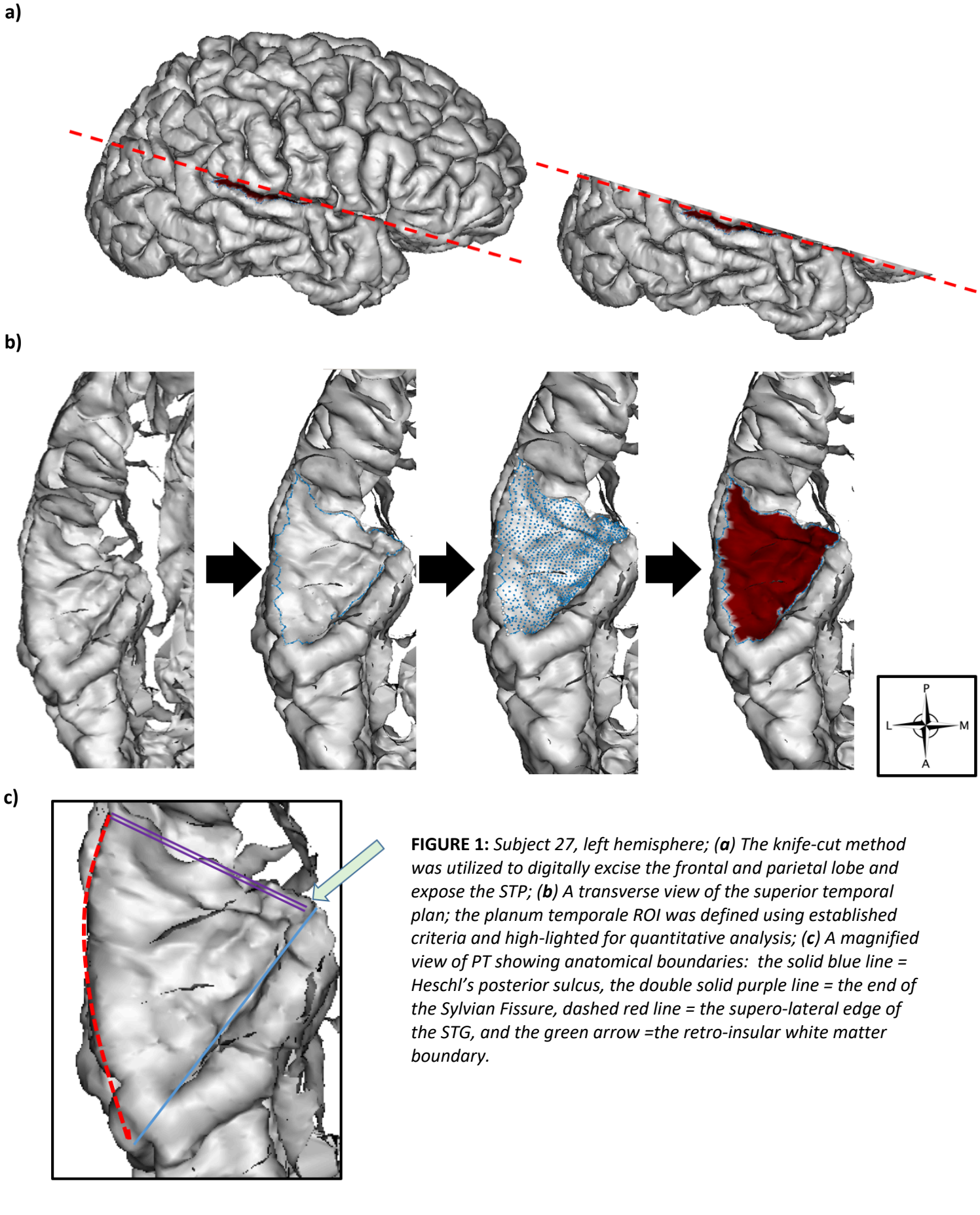

FIGURE 1: *Subject 27, left hemisphere; (**a**) The knife-cut method was utilized to digitally excise the frontal and parietal lobe and expose the STP; (**b**) A transverse view of the superior temporal plan; the planum temporale ROI was defined using established criteria and high-lighted for quantitative analysis; (**c**) A magnified view of PT showing anatomical boundaries: the solid blue line = Heschl's posterior sulcus, the double solid purple line = the end of the Sylvian Fissure, dashed red line = the supero-lateral edge of the STG, and the green arrow =the retro-insular white matter boundary.*

Heschl's Gyri Variations

Examples for the first three Heschl's Gyri variations are listed in **FIGURE 2a-c.**

Single: This variation is defined as a single gyrus on the STP that is bordered anteriorly by Planum Polare, posteriorly by PT, laterally by the supero-lateral boundary of the STG and medially by retroinsular white matter.

Common stem Duplication (CSD): A CSD is defined as a partial duplication of HG separated by a sulcus that extends anterolaterally to posteromedially and separates Heschl's gyri but does not extend completely to the medial retroinsular border. This sulcus has also been referred to as "Beck's Intermedius" or "Intermedius of Beck" (St. George et al., 2017; Leonard et al., 1998; Rademacher et al., 1993).

Complete Duplication (CPD): This variant is defined as two HG separated by an intermedial sulcus that extends from the medial retroinsular white matter border, and courses posteromedially to anterolaterally. The sulcus is at least 1/3 the length of the Heschl's gyri (St. George et al., 2017; Leonard et al., 1998; Rademacher et al., 1993).

Triple Heschl's Gyri: Less commonly observed, this variant is defined as the presence of three Heschl's gyri. Given its rarity, descriptions of the sulci separating each HG is sparse in the literature, but includes both sulci that do and do not extend from the medial retro-insular white

matter border, as described in the CSD and CPD, respectively (Marie et al., 2015; Campain & Minckler, 1976).

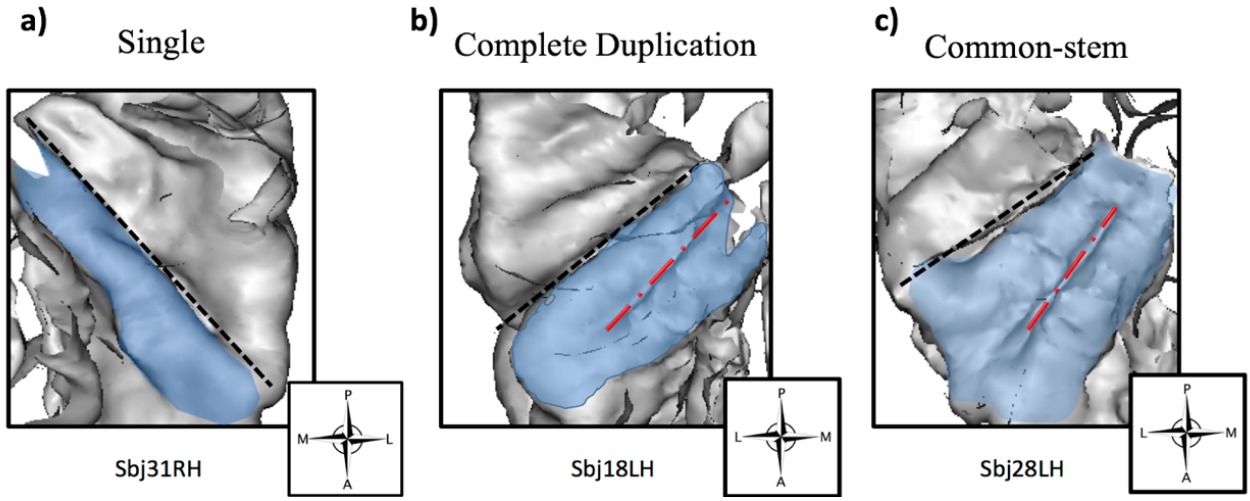

FIGURE 2: *Examples of Heschl's Gyrus variations, in blue high-lighted area, on a 3D cortical mesh manifesting as* ***(a)*** *single HG,* ***(b)*** *full posterior complete duplication,* ***(c)*** *a common-stem duplication. The red barred line indicates Beck's Intermedius and the black barred line indicates Heschl's posterior most sulcus, the anterior border of PT.*

Posterior Sylvian Fissure Variations

Morphological variations of the posterior SF were identified using criteria set forth by St. George and colleagues (2016) and incorporated into this study. Variations included: *Posterior Ascending Ramus* (PAR), *Posterior Descending Ramus* (PDR), *Straight Posterior Extension* and *Other*, which included Bifurcations and Trifurcations.

Morphological Shape of Planum Temporale

Pie shaped- Defined as the presence of three vertices, edges and angles that form a triangle-like structure. The anterior and posterior edges of PT course postero-medially and come to a point that meets at the medial retro-insular white matter border. **See FIGURE 3a**.

Trapezoid shaped- Defined as the presence of four vertices, edges and angles that form a quadrilateral-like structure. The anterior and posterior edges of PT course postero-medially and medial vertices are connected by an edge that runs parallel to the retroinsular white matter boundary. The lateral edge is demarcated by the supero-lateral boundary of the STG and is larger compared to the medial edge. The medial edge will be less than 50% of the length of the lateral edge. **See FIGURE 3b**.

Rectangular Shaped- Defined as the presence of 4 vertices, edges and angles. Similar to the trapezoid classification, the anterior and posterior edges course postero-medially. However, the medial edge, which is demarcated by the retroinsular white matter, is greater than 50% of the length of the lateral edge, which is marked by the supero-lateral boundary of the STG. **See FIGURE 3c.**

None- Defined as not fitting any of the above mentioned gross morphological classifications. Specifically, defined as the absence of PT using typical classification for Heschl's Gyri and Posterior Sylvian Fissure. **See FIGURE 3d**.

Statistical Analysis

All statistical analyses were made using R for Mac OS X 10_15_0, version 1.2.5001 (R Core Team, 2019) with the two-tailed statistical significance level set at $p < .05$. A Pearson's chi-squared test was performed to make between-group comparisons of categorical data, specifically, the number of occurrence for each PT classification was compared between hemispheres and by gender. Linearity, homogeneity (Levene's $F(5, 85) = 1.15$, $p = .34$), homoscedasticity , and normality were all met. A two-way analysis of covariance (ANCOVA)

was used to analyze the interaction between PT morphological shape and hemisphere on overall mean surface area of PT after controlling for estimated total intracranial volume (eTIV), age and sex as covariates. Lastly, a Spearman correlation analysis was implemented to examine the associations between PT classifications and demographic variables, including gender, age and hemisphere. The level of significance was set at $p<.05$.

Results

A total of four PT configurations were identified (**see FIGURE 4a**):

1) Pie-shaped [45%]- (45/100 hemispheres)
2) Trapezoid-shaped [27%] – (27/100 hemispheres)
3) Rectangular-shaped [19%]- (19/100 hemispheres)
4) None [9%] - (9/100 hemispheres)

Frequency of Occurrence Comparisons

Overall, PT was shown to manifest, in order of most common to least common, in a "*Pie-shaped*", "*Trapezoid-shaped",* "*Rectangular-shaped*" and "*None*" configuration. There were non-significantly more "*Pie-shaped*" PT configurations occurring in the right hemisphere and non-significantly more "*Trapezoid-shaped*" and *"Rectangular-shaped*" PTs occurring in the left hemisphere **(see FIGURE 5a)**. The "*None*" PT classification was observed to significantly occur more in the right hemisphere compared to the left hemisphere ($X^2(1,N=9)= 5.44$, $p=.02$, $\phi=0.78$). In **FIGURE 6a**, the number of occurrence of PT classifications was examined with respect to sex. There were non-significantly more "*Pie-shaped*" PTs in males and non-significantly more "*Rectangular-shaped*" PTs in females. The *"Trapezoid-shaped"* PT was shown to occur significantly more in females ($X^2(1,N=27)= 6.26$, $p=.01$, $\phi=0.48$) and the "*None"* PT classification was found to occur significantly more in males ($X^2(1,N=9)= 5.44$, $p=.02$, $\phi=0.78$).

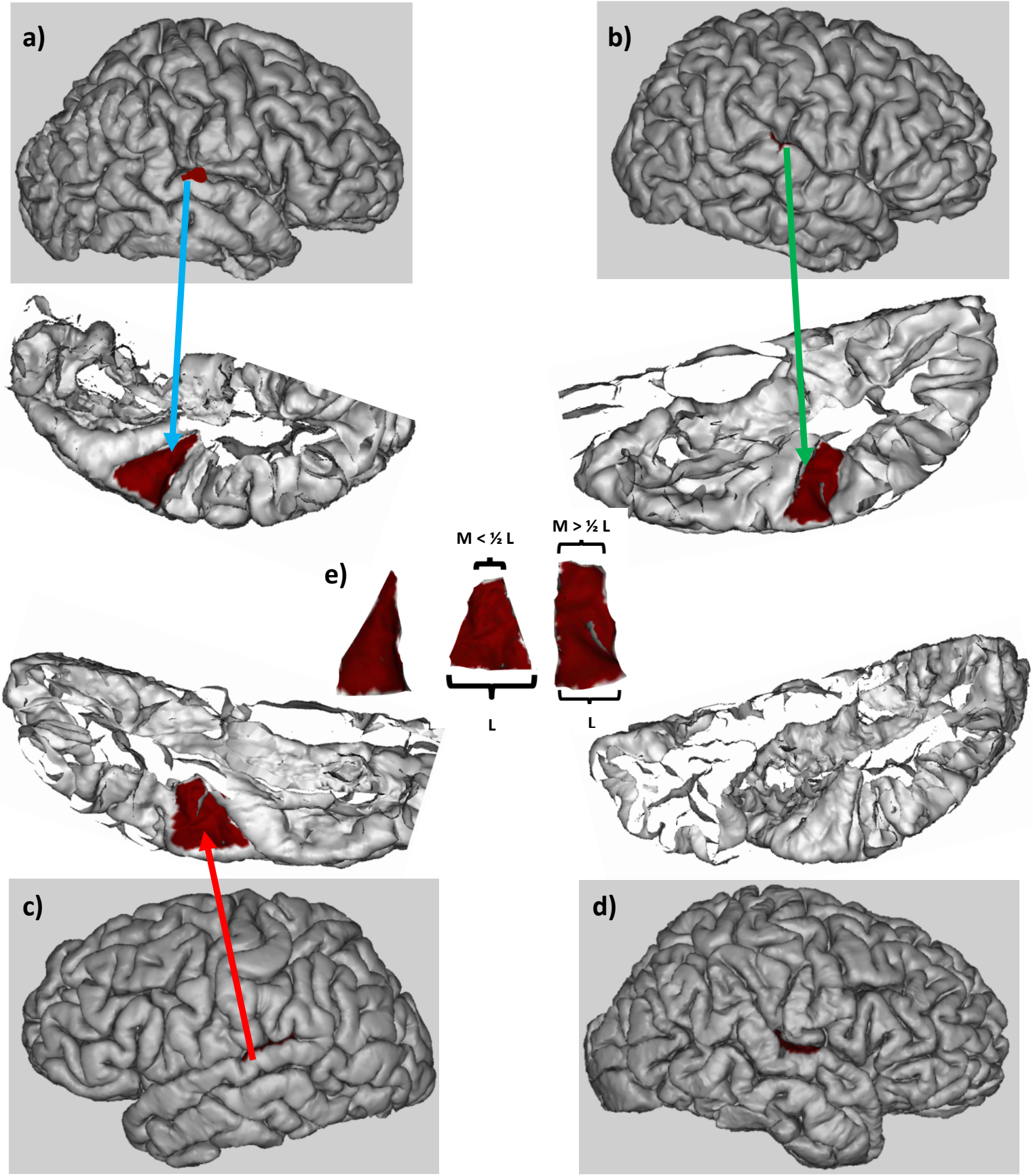

FIGURE 3: ***(a-d)*** *indicate the lateral and corresponding transverse views of the the "Pie", "Rectangular", "Trapezoid" and "None" PT categories, respectively. The red highlighted areas on the transverse slice indicate PT's expanse used for quantification;* ***(e)*** *Magnified images of the PT categories. The term "M"= the medial edge and "L" = Lateral edge of PT.*

a)

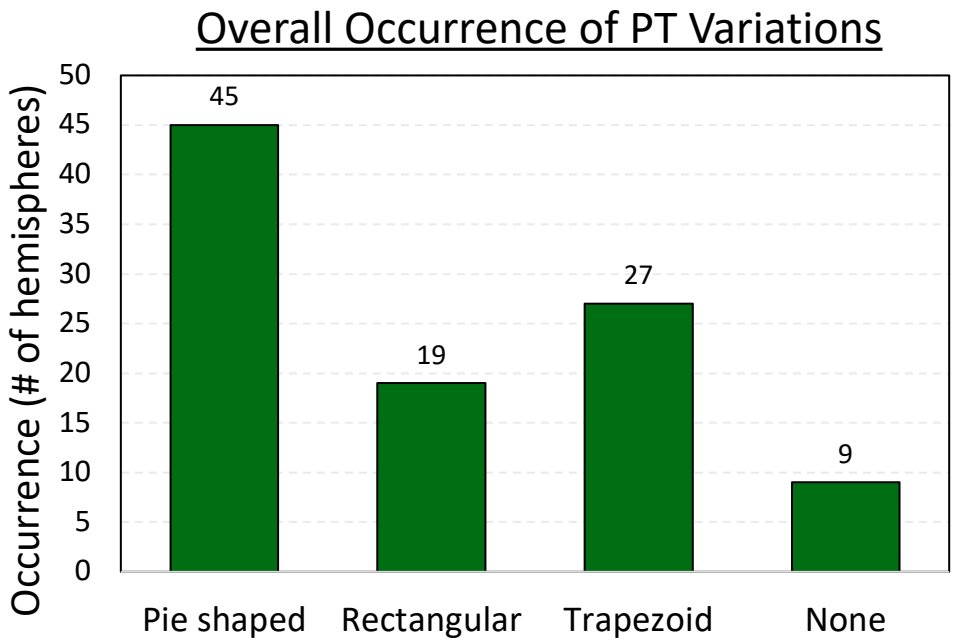

b)

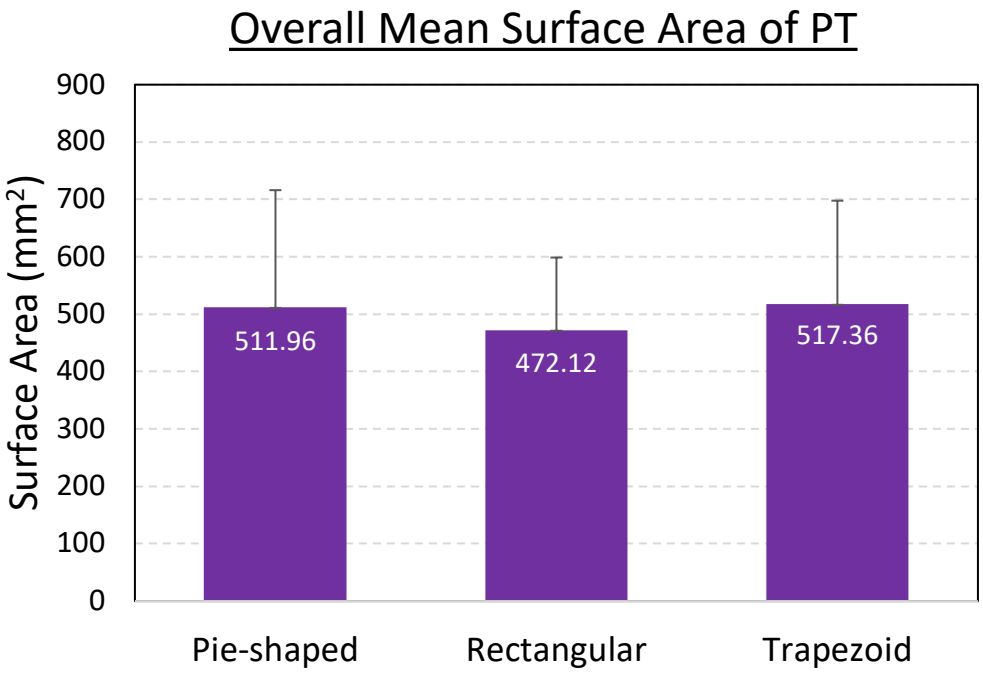

FIGURE 4: * = *p*<.05. **(a)** Describes the number of occurrence of each PT category. The most common PT category was the "*Pie-shaped"* category. **(b)** This describes the mean overall surface area of each PT category. The "Trapezoid-shaped" category exhibited the greatest overall adjusted mean surface area.

a)

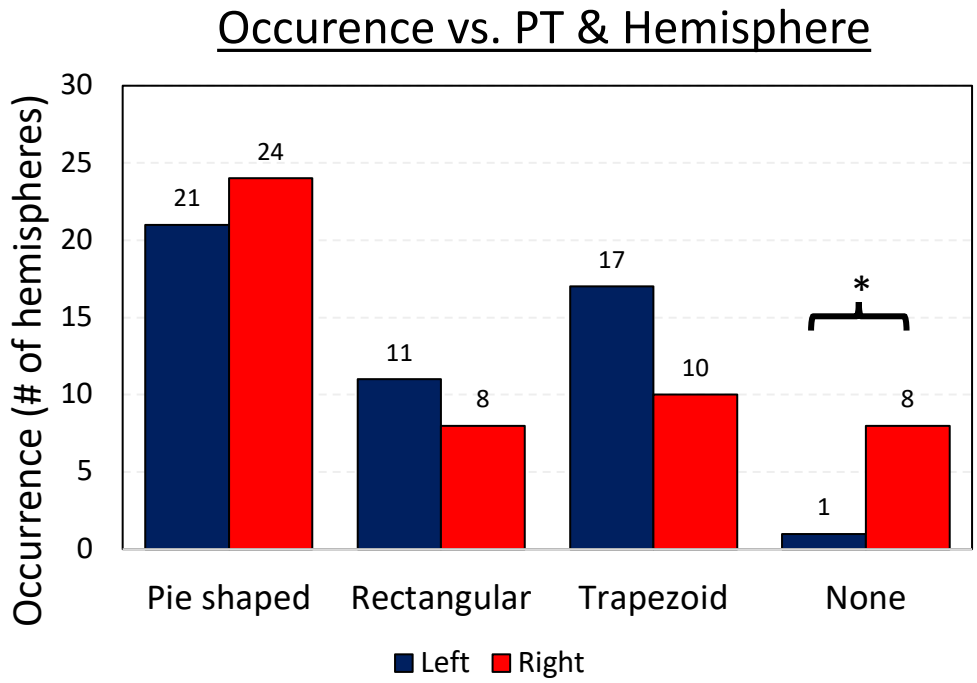

b)

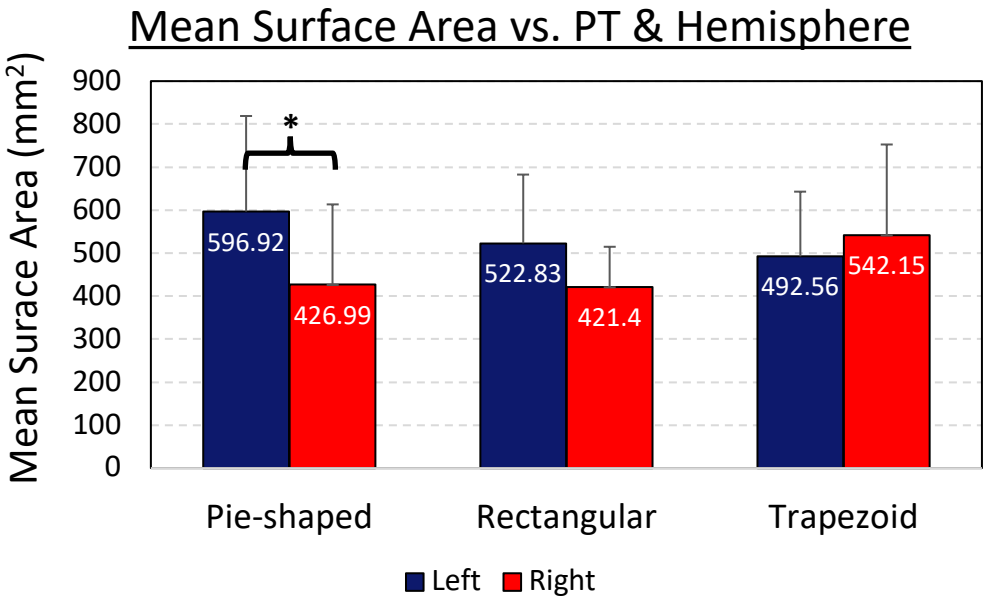

FIGURE 5: * = *p*<.05; **(a)** Describes the number of occurrence of each PT variation by hemisphere. There was significantly more "*None*" PTs in the right hemisphere compared to the left. **(b)** This describes the mean overall adjusted surface area of each PT variant by hemisphere. There was a significantly greater overall mean surface area for the left hemisphere of the "*Pie-shaped*" category.

a)

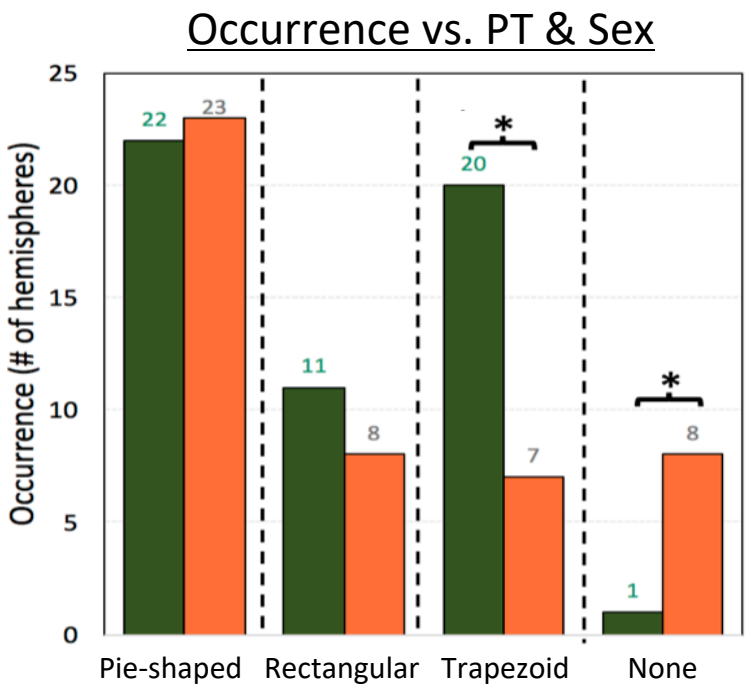

b)

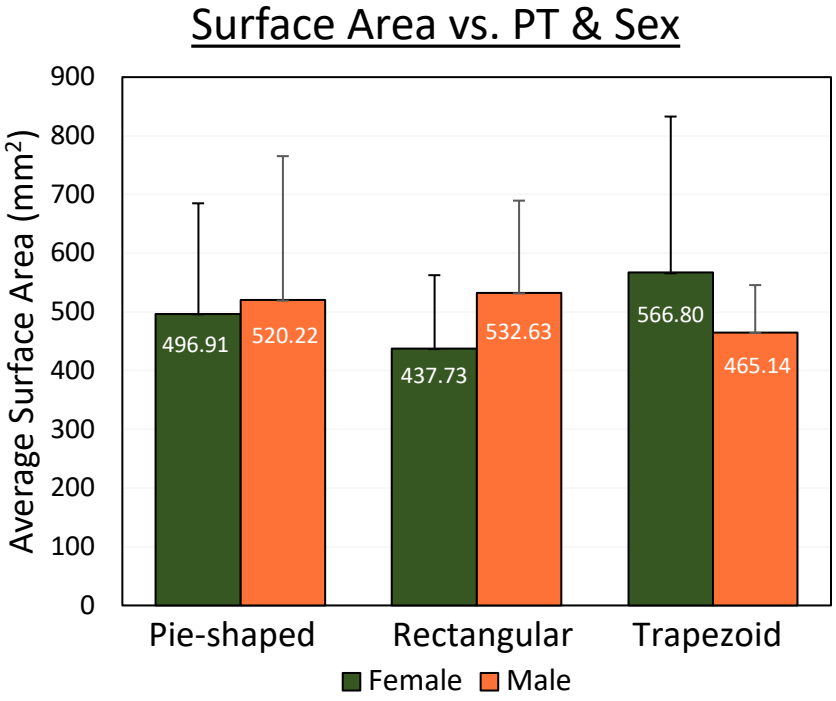

FIGURE 6: * = *p*<.05; **(a)** There was significantly more *"Trapezoid-shaped"* PTs in females compared to males and and significantly more "*None*" PTs occurring in males compared to females; **(b)** Males were observed to have larger mean adjusted surface area for "*Pie-shaped*" and "*Rectangular*" PTs, but not for the "*Trapezoid*" shaped PTs. These differences were non-significant.

Surface Area Comparisons

Next, the mean surface area of each PT classification was examined overall **(FIGURE 4b)** , by hemisphere **(FIGURE 5b)** and then by sex **(FIGURE 6b).** Both the right and left hemispheres were collapsed for the overall condition and revealed no statistically significant difference between PT classification and overall mean surface area. Adjusted mean surface areas of measurable PT configurations, in order from greatest to least, were: 517.36 mm^2 for "*Trapezoid-shaped*" (*n*=27*),* 511.96 mm^2 for *"Pie-shaped*" (*n=45),* and 472.12 mm^2 for "*Rectangular-shaped*" (*n=19)*. The fourth category, "*None*" (*n*=9), was not calculable. Both *"Pie-shaped"* and "*Rectangular-shaped"* PT classifications were larger in the left hemisphere compared to the right hemisphere, with statistical significance only for the "*Pie-shaped*" classification ($F(2,90)=5.719$, $p=.019$, $\eta^2 = 0.079$). The *"Trapezoid-shaped"* PT demonstrated a non-significantly larger mean surface area in the right hemisphere compared to the left hemisphere. In terms of sex, there were no statistically significant differences even when eTIV was accounted for as a covariate **(FIGURE 6)**. Males had non-significantly larger mean surface areas for the "*Pie-shaped*" and "*Rectangular shaped*" PT categories and females had a non-significantly larger mean surface area for the "*Trapezoid-shaped*" PT category.

Correlation

There were no significant correlations detected between PT classification and age or sex ($p > .05$). The left hemisphere was observed to positively correlate with larger PT surface areas ($r=0.26$, $p=.01$).

Discussion

The primary finding is that PT does indeed manifest in various morphological shapes, not just "*Pie-shaped*". A total of four PT configurations were identified, in order of most common to least common: (1) Pie-shaped, (2) Trapezoid-shaped, (3) Rectangular-shaped and (4) None.

Prediction #1: The PT will manifest in various morphological shapes, with "Pie-shaped" being the most common.

As previously stated, there were four total PT configurations noted. The "*Pie-shaped*" PT classification was demonstrated to occur most frequently in 45% (45/100 hemispheres) of examined brain images, which is consistent with our initial hypothesis. Because this is the most common variant of PT, it may have been misconstrued over time as the only variant; a notion clearly prevalent in the literature **(TABLE 1)**. The finding of multiple PT morphological variations has huge implications in terms of navigating the complex topography of the superior temporal plane; specifically, the differentiation between PT and HG. For example, if students, neuroanatomists or even clinicians rely on the incorrect assumption that PT is always "*Pie-shaped*", they may misidentify or completely overlook the correct neuroauditory substrate. Additionally, this PT taxonomy may also aid in interpretation of functional imaging studies and auditory electrophysiologic studies that focus on this auditory cortical region. More accurate identification of PT from HG can contribute to a better understanding of how these structures process complex auditory stimuli, both separately and in tandem.

TABLE 3: ANCOVA results using PT morphological shape and Hemisphere as grouping variables

	Sum of Squares	Df	Mean Square	F-value	p-value	Partial η^2
eTIV	1486	1	1486	0.04	0.84	0.001
Sex	2211	1	211	0.06	0.8	0.001
Age	25	1	25	0.001	0.98	0.000
PT	14747	2	7373	0.211	0.81	0.010
Hem	199088	1	199088	5.713	**0.02***	0.070
PT:Hem	164429	2	82215	2.362	0.1	0.050

* *statistical significance at the p<.05 level. DV = mean surface area, IV = PT morphology and Hemisphere.*

TABLE 4: Post-hoc multiple comparisons using Tukey HSD

PT_ morph	Hemisphere	Mean Surface Area (mm^2)	Mean Difference (I-J)	Std. Error	T-value	sig.	Cohen's D
Pie-shaped	left (I)	596.92 (222.01)					
	right (J)	426.99 (186.36)	169.93	66.57	2.436	**0.02***	0.79
Rectangular	left (I)	522.83(159.87)					
	right (J)	421.40(93.37)	101.43	67.35	1.28	0.22	0.74
Trapezoid	left (I)	492.56(150.43)					
	right (J)	542.15(210.51)	-49.59	91.62	–.61	0.55	0.17

* *statistical significance at the p<.05 level.*

Prediction #2: New PT classifications will have larger surface areas in the left hemisphere.

Our initial prediction was incorrect. Both the *"Pie-shaped"* and *"Rectangular-shaped"* PT's exhibited larger left hemisphere mean surface areas with the *"Trapezoid-shaped"* PT demonstrating a larger right mean surface area. However, only the left *"Pie-shaped"* PT exhibited statistically significantly results ($F(1,85)= 5.719, p=.019, \eta^2= 0.08$). This is consistent with previous post-mortem (Galaburda et al., 1987; Teszner et al., 1972; Kopp et al., 1977; Falzi et al., 1982; Nikkuni et al., 1981) and imaging studies (Foundas et al., 1994; Barta et al., 1995; Foundas et al., 1995; Steimetz & Galaburda, 1991; Kulynyc et al., 1993; St. George et al., 2017)

which have observed this same left greater than right PT asymmetry in normal intact brains. One explanation for this leftward size asymmetry in PT is its implication in being involved with speech processing networks, given its proximal location to known peri-sylvian cortical language areas and as evidenced by functional imaging studies (Hickock et al., 2009; Obleser & Kotz, 2009; Price et al., 2010, Deschamps & Tremblay, 2014). This leftward lateralization is explained on a microscopic level as well. In a study previously mentioned in the introduction by Ocklenburg et al., (2017), greater *in-vivo* neuronal density was demonstrated in the left PT compared to the right PT. These authors then used electroencephalography to measure the event-related potential N1, whose neural generator site is believed to be in the posterior superior temporal plane (Godey et al., 2001; Wolpaw & Penry, 1975), and demonstrated a decreased latency for the left hemisphere C5 electrode compared to the right hemisphere C4 electrode in response to dichotically presented auditory stimuli. This implies that the left PT is larger because it is predisposed to handle more complex auditory stimuli, such as speech, at a faster rate.

It is our view that auditory temporal processing abilities necessitates initial spectro-temporal decomposition of complex auditory signals that sub-serves overall speech processing abilities. Auditory temporal processing is a general term used to describe sub-processes including: temporal ordering, temporal resolution, temporal integration and temporal masking (Musiek et al., 2005). Tests examining temporal ordering and temporal resolution abilities are used more commonly for clinical and research purposes when examining the integrity of the central auditory nervous system. As previously stated, the PT has been shown to be active during auditory temporal processing tasks, specifically temporal ordering, such as duration

pattern and frequency pattern tests (Griffiths et al., 1999; Binder et al., 2000; Hall et al., 2002). Comparatively, there are fewer imaging studies examining PT activation in response to auditory temporal resolution tasks, an individual's ability to detect rapid changes in the envelope of a sound over time. In an fMRI study by Zaehle, Wüstenberg, Meyer and Jäncke (2004), subjects performed a gap-detection task and consonant-vowel syllable discrimination task in which they had to match the test stimulus with the correct target probe stimulus. For both conditions, the results demonstrated overall greater activation of the left HG and PT compared to their right homologues, with significantly greater activation of PT compared to HG. Additionally, there was significant overlapping activation patterns of the non-speech condition with speech condition. The authors concluded that the ability for rapid auditory temporal resolution is lateralized to the left superior temporal plane. Another way to evaluate temporal resolution is by utilizing amplitude modulated and frequency modulated auditory signals. In another fMRI study by Hall, Haggard, Akeroyd, et al. (2000), subjects passively and actively listened to binaurally presented frequency modulated and amplitude modulated pure tones. The results also demonstrated bilateral activation of HG, PT and STG with enhanced activation of left PT during the active condition. While these studies provide insight into what cortical areas are active during auditory temporal processing tasks, they do not evaluate quantitative measures, such as surface area or volume, of HG and PT. Because of this, any correlation between auditory temporal processing task performance and size asymmetry of cortical auditory structures cannot be confidently commented upon and should be further evaluated in future studies.

3rd Prediction: PT classifications with more edges and vertices will exhibit greater surface areas.

This prediction was incorrect. In this current study, the order from greatest to least overall mean surface area for PT classifications was: "*Trapezoid- shaped*" (517.36 mm^2), "*Pie-shaped*" (511.96 mm^2) and "*Rectangular-shaped*" (472.12 mm^2). The overall mean surface area between PT classifications, regardless of hemisphere, were comparable. This is a surprise, as it was anticipated that PT classifications with more edges and vertices would exhibit greater mean surface areas due to extension of the medial insular white matter boundary. However, upon further investigation, it would seem that the surface area is more dependent on both the lateral width and medial depth of the measured structure.

4th Prediction: There will be no significant sex differences in terms of PT variation occurrence, but males will exhibit overall greater PT surface area compared to females.

Our third prediction was both incorrect and correct. Contrary to our hypothesis regarding PT number of occurrence, the "*Trapezoid-shaped*" PT variant was demonstrated to be significantly more prevalent in females compared to males ($X^2(1,N=27)= 6.26$, $p=.01$, $\phi=0.48$). Although non-significant, it is also worth mentioning that the "*Trapezoid-shaped*" PTs also occurred more frequently in the left hemisphere. Additionally, the "*None*" PT variant was also demonstrated to occur significantly more in males ($X^2(1,N=9)= 5.44$, $p=.02$, $\phi=0.78$). Functional sexual dimorphism has been observed in cortical auditory regions. In a PET study by Ruytjens, Georgiadis, Holstege, et al. (2007), females were observed to have greater regional cerebral blood flow (rCBF) activation of the primary auditory and secondary auditory areas when

passively attending to white noise compared to music stimuli. They purport that this difference in rCBF pattern is modulated by differences in frontal-temporal connections, specifically attention, given their concurrent finding of decreased right prefrontal activity for male participants. In another PET imaging study examining gender differences of rCBF in a silently-mouthed versus verbally-spoken lip reading task, Ruytjents, Albers, Dijk, et al. (2007) observed that only females exhibited significantly greater rCBF activation for the left primary auditory cortical region when instructed to internally repeat silently-mouthed numbers. Similarly, they concluded that the contrast in activation patterns between sex is associated with differences in cortical processing networks used for auditory information, even anticipatory and internally represented auditory stimuli. It is possible that neuroanatomical differences of PT shape/form found in the present study serve as underpinnings of these observed sexual dimorphic differences in the frontal-temporal cortical processing patterns. However, this is speculation that requires more in depth studies comparing auditory function with macroscopic PT shape, and not just primary auditory areas.

Additionally, males were demonstrated to have non-significantly larger overall mean surface areas for the "*Pie-shaped*" and the "*Rectangular-shaped*" PTs, but not the "*Trapezoid-shaped*" PT. This supports the latter part of our 4th hypothesis, that males would generally have larger mean surface area measurements across all PT variants. Given the propensity for the average normal male brain to be larger can result in greater leftward lateralization of PT compared to females (Stein et al., 2012; Good et al., 2001; de Courten-Myers, 1999; Shapleske et al., 1999). The neurobiologic and molecular bases for cortical asymmetries between homologous neural substrates, including PT, is not well understood. In a study by Lombard,

Ashwin, Auyeung et al., (2012), higher fetal testosterone levels were observed to positively predict greater cortical grey matter volume in various brain regions, including PT. The exact mechanistic pathways that underlie hormonal and genetic modulation are still being researched. In a unique study examining possible genetic determinants of PT asymmetry, Guadalupe et al. (2014) found an association between enhancement of single-nucleotide polymorphisms, or alterations in single nucleotides at specific locations, and the size asymmetry for PT. They conceive that sexual dimorphisms in PT are modulated and regulated, downstream, by pathways involved in steroid metabolic processes and steroid hormone receptor activity.

A surprising finding was the "*None"* PT classification and it preponderance to significantly occur in the right hemisphere and in males ($X^2(1,N=9)= 5.44$, $p=.02$, $\phi=0.78$). One explanation is that in these cases, PT portions may extend with the Posterior Sylvian Fissure (PSF): either dorso-posteriorly in tandem with PAR or caudo-posteriorly in cases with descending rami. This would be consistent with cytoarchitectonic studies that demonstrated that parakoniocortex, or auditory association cortex, is individually variable and observed to spill over onto temporal-parietal convexity and follow the PSF (Galaburda et al., 1978; Witelson et al., 1995; Shapleske et al., 1999). Because the criteria used in this study defined the posterior border of PT as the beginning of the PAR, or the termination of the horizontal SF, planum temporale would not have been accounted for. Another, less likely, possibility is that PT truly does not exist in these cases. This could result either as a normal morphological variant found predominantly in the right-hemispheres of males or it could be related to an unsolicited disorder or pathology. Because these brain images were obtained from an open access

neuroimaging repository, only a limited subset of patient data and history are readily accessible. Such limited information included age, sex, handedness, and neurologic integrity. However, the term "neurologic integrity" is ambiguous and it is unclear if this refers only to confirmed neurological structural lesions, such as cerebral vascular accidents, or encompasses broader neurological pathologies, such as dyslexia, multiple sclerosis, or traumatic brain injury. If PT is missing, subjects should be evaluated via behavioral central auditory testing or late auditory evoked potentials to determine if there is a functional consequence. If there is a functional deficit on testing, PT may truly be absent. However, if there is no functional deficit, then PT is most likely there, but not visualizable based on our criteria. In future studies, more patient information and data would be required to make sure these PT classifications, specifically the "*None"* category, are reflective of normal population.

Study Limitations and Future Goals

In this section, other possible study limitations and future goals will be addressed. One potential limitation that has been continually addressed in imaging research is how reliable the accuracy of *in-vivo* quantitative measurements reflects true anatomical measurements. In a unique study comparing radiologic versus anatomic surface area measurements on 10 post-mortem brains, Steimetz et al. (1989) demonstrated that planimetric measurements made by MR did not significantly differ from the same measurements made on the actual cadaver brains. In a similar study by Kulynych et al. (1993), 3D surface rendering of MRI sections offered greater inter-rater reliability and improved validity for PT identification and subsequent quantitative measurements compared to to the same measurement made on 2D MRI images. If there is a

small degree of error in surface area, it is likely attributed to the software used to define the PT area. In BrainVISA anatomist, an ROI texture area is defined using a closed series of selected points; points that can be specified to hug the nearest sulcus. As a result, it is possible that miniscule portions of the defined PT ROI may not be incorporated into the surface area measurements, but overall does not affect interpretation of results.

More information should also be collected from the participants. Since these brain images were obtained from open-access neuroimaging repositories. Only limited information (age, gender, neurologically intact, handedness) was accessible. Future studies should include information regarding hearing status and presence of any learning or language disabilities.

Another issue that has been brought up is the comprehensiveness of the PT morphological taxonomy. The present authors of this article contend that although 50 brains, 100 hemispheres, is a decently moderate sized sample, there may exist other, rarer morphological variations of PT that were not represented in this study.

In future studies, a larger sample size should also be used to (1) add to and replicate morphological variations found in this study, and (2) obtain more accurate occurrence of these PT morphological variations in normally intact brains. An additional study that may prove enlightening is examining occurrence of PT morphological variations in pathological brains to see if there are any differences.

Conclusion

Planum temporale is demonstrated to be morphologically variable across individuals and does not simply occur in just a "*Pie-shaped*" configuration. The taxonomy put forth will aid neuroanatomists, clinicians and students in terms of differentiation of the sometimes complex topography of the STP. It also takes the initial step in describing the morphological variation in normal intact brains. This can provide an additional dimension to describe and compare the anatomy of disordered brains with normal brains and contribute to better interpretation of pathological effects, auditory evoked potentials, and behavioral auditory tests which focus on this cortical auditory region.

References

Altarelli, I., Leroy, F., Monzalvo, K., Fluss, J., Billard, C., Dehaene-Lambertz, G., ... & Ramus, F. (2014). Planum temporale asymmetry in developmental dyslexia: Revisiting an old question. Human brain mapping, 35(12), 5717-5735.

Barta, P. E., Petty, R. G., McGilchrist, I., Lewis, R. W., Jerram, M., Casanova, M. F., ... & Pearlson, G. D. (1995). Asymmetry of the planum temporale: methodological considerations and clinical associations. Psychiatry Research: Neuroimaging, 61(3), 137-150.

Barta, P. E., Pearlson, G. D., Brill, L. B., Royall, R., McGilchrist, I. K., Pulver, A. E., ... & Petty, R. G. (1997). Planum temporale asymmetry reversal in schizophrenia: replication and relationship to gray matter abnormalities. American Journal of Psychiatry, 154(5), 661-667.

Binder, J.R., Frost, J.A., Hammeke, T.A., Bellgowan, P.S.F., Springer, J.A., Kaufman, J.N., & Possing, E.T. (2000) Human temporal lobe activation by speech and nonspeech sounds. *Cereb. Cortex 10,* 512–528

Bloom, J. S., Garcia-Barrera, M. A., Miller, C. J., Miller, S. R., & Hynd, G. W. (2013). Planum temporale morphology in children with developmental dyslexia. Neuropsychologia, 51(9), 1684-1692.

Bremmer, B., Schlack, A., Shah, N.J., Zafiris, O., Kubischik, M., Hoffmann, K.P., Ziles, K., & Fink, K.R. (2001). Polymodal motion processing in posterior parietal and premotor cortex. *Neuron, 29,* 287-296.

Buckener, R.L., Head, D., Parker, J., Fotenos, A.F., Marcus, D., Morris, J.C., & Snyder, A.Z

(2004). A unified approach for morphometric and functional data analysis in young, old, and demented adults using automated atlas-based head size normalization: reliability and validation against manual measurement of total intracranial volume. *NeuroImage, 23,* 724-738.

Campain, R. & Minckler, J.A. (1976). A note on the gross configuration of the human auditory cortex. *Brain Lang, 3,* 318-323.

Da Costa, S., van der Zwaag, W., Marques, J.P., Frackowiak, R.S., Clarke, S. & Saenz, M. (2011). Human primary auditory cortex follows the shape of Heschl's gyrus. *J Neurosci, 31,* 14067-14075.

Dale, A. M., Fischl, B., & Sereno, M. I. (1999). Cortical surface-based analysis: I. Segmentation and surface reconstruction. Neuroimage, 9(2), 179-194.

De Courten-Myers, G.M. (1999). The human cerebral cortex: gender differences in structure and function. *Journal of Neuropathology and Experimental Neurology, 58(3),* 217-226.

De Martino, F., Moerel, M., Xu, J., van de Moortele, P.F., Ugurbil, K., Goebel, R., Yacoub, E., & Formisano, E. (2015). High-resolution mapping of myeloarchitecutre in vivo: Localization of auditory areas in the human brain. *Cereb Cortex, 25(10),* 3394-405.

Deschamps, I. & Tremblay, P. (2014). Sequencing at the syllabic and supra-syllabic levels during speech perception: An fMRI study. *Front Hum Neurosci, 8,* 492-5.

Dronkers, N.F., Wilkins, D.P., Van Valin Jr, R.D., Redfern, B.B. & Jaeger, J.J. (2004). Lesion analysis of the brain areas involved in language comprehension. *Cognition, 92(1)*, 145-177.

Foundas, A. L., Leonard, C. M., & Heilman, K. M. (1995). Morphologic cerebral asymmetries

and handedness: The pars triangularis and planum temporale. Archives of Neurology, 52(5), 501-508.

Falkai, P., Bogerts, B., Schneider, T., Greve, B., Pfeiffer, U., Pilz, K., ... & Ovary, I. (1995). Disturbed planum temporale asymmetry in schizophrenia. A quantitative post-mortem study. Schizophrenia research, 14(2), 161-176.

Falzi, G., Perrone, P., & Vignolo, L.A. (1982). Right-left asymmetry in the anterior speech region. *Archives of Neurology, 39,* 239-240.

Foundas AL, Leonard CM, Gilmore R, Fennell E, & Heiman K (1994). Planum temporale asymmetry and language dominance; *Neuropsychologia, 37(10),* 1225-1231.

Galaburda AM, Corsiglia J, Rosen GD & Sherman GF (1987). Planum temporale asymmetry, reappraisal since Geschwind and Levitsky. *Neuropsychologia, 25(6),* 853-868.

Geschwind N & Levitsky W (1968). Human Brain: left-right asymmetries in temporal speech region, *American Association for the Advancement of Science, 161(3837),* 186-187.

Godey, B., Schwartz, D., de Graaf, J.B., Chauvel, P., & Liégos-Chauvel, C. (2001). Neuromagnetic source localization of auditory evoked fields and intracerebral evoked potentials: a comparison of data in the same patients. *Clinical Neurophysiology, 112,* 1850-1859.

Good, C.D., Johnstrude, I., Ashburn, J., Henson, R.N., Friston, K.J., & Frackowiak, R.S. (2001). Cerebral asymmetry and the effects of sex and handedness on brain structure: a voxel based morphometric analysis of 465 normal adult human brains. *NeuroImage, 14(3),*

685-700.

Griffiths, T.D. Johnsrude, I., Dean, J.L., & Green, G.G. (1999) A common neural substrate for the analysis of pitch and duration pattern in segmented sound?, *Neuroreport, 10(18),* 3825-30.

Griffiths, T.D. & Warren, J.D. (2002). The planum temporale as a computational hub. *Trends Neurosci, 25 (7),* 348-353.

Guadalupe, T., Zwiers, M.P., Wittfeld, K., Teumer, A., Vasquez, A.A., Hoogman, M., Hagoort, P., Fernandez, G., et al. (2015). Asymmetry within and around the human planum temporale is sexually dimorphic and influenced by genes involved in steroid hormone receptor activity. *Cortex, 62,* 41-55.

Hackett, T.A., Preuss, T.M., & Kass, J.H. (2001). Architectonic identification of the core region in auditory cortex of macaques, chimpanzees, and humans. *Journal of Comparative Neurology, 441,* 197-222.

Hall, D.A., Haggard, M.P., Akeroyd, M.A., Summerfield, A.Q., Palmer, A.R., Elliott, M.R., & Bowtell, R.W. (2000). Modulation and task effects in auditory processing measured using fMRI. *Human Brain Mapping, 10,* 107-119.

Hall, D.A.; Johnsrude, I.S., Haggard, M.P., Palmer, A.R., Akeroyd, M.A. & Summerfield, A.Q. (2002) Spectral and temporal processing in human auditory cortex. *Cereb. Cortex 12*, 140–149

Hall, D.A., Hart, H.C., & Johnstrude, I.S. (2003). Relationships between human auditory cortical structure and function. *Audiology & Neurotology, 8,* 1-18.

Hasan, A., Kremer, L., Gruber, O., Schneider-Axmann, T., Guse, B., Reith, W., ... & Wobrock,

T. (2011). Planum temporale asymmetry to the right hemisphere in first-episode schizophrenia. Psychiatry Research: Neuroimaging, 193(1), 56-59.

Hashimoto, R., Homae, F., Nakajima, K., Miyashita, Y., & Sakai, K.L. (2000) Functional differentiation in the human auditory and language areas revealed by a dichotic listening

task. *NeuroImage 12,* 147–158

Hickok, G., Okada, K., & Serences, J.T. (2009). Area spt in the human planum temporale supports sensory-motor integration for speech processing. *J. Neurophysiol., 101*, 2725–2732.

Hickock, G., & Saberi, K. (2012). Redefining the functional organization of the planum temporale region: Space, objects, and sensory-motor integration. *The Human Auditory Cortex,* 333-350.

Hugdahl, K., Heiervang, E., Nordby, H., Smievoll, A. I., Steinmetz, H., Stevenson, J., & Lund, A. (1998). Central auditory processing, MRI morphometry and brain laterality: applications to dyslexia. Scandinavian Audiology, 27(4), 26-34.

Kasai, K., Shenton, M. E., Salisbury, D. F., Hirayasu, Y., Onitsuka, T., Spencer, M. H., ... & McCarley, R. W. (2003). Progressive decrease of left Heschl gyrus and planum temporale gray matter volume in first-episode schizophrenia: a longitudinal magnetic resonance imaging study. Archives of general psychiatry, 60(8), 766-775.

Kim, W.J. & Paik, N.J. (2014). Lesion localization of global aphasia without hemiparesis by overlapping of the brain magnetic resonance images. *Neural Regen Res, 9(23),* 2081-2086.

Koelsch, S., Schulze, K., Sammier, D., Fritz, T., Müller, K., & Gruber, O. (2009). Functional architecture of verbal and tonal working memory: an FMRI study. *Hum Brain Mapp, 30(3),* 859-873.

Kopp, N., Michel, F., Carrier, H., Biron, A., & Duvillard, P. (1977). Etude de certaines asymmetries hemispheriques du cerveau humain. *Journal of the Neurological Sciences, 34,* 349-363.

Kulynych, J.J., Vladar, K., Jones, D.W., & Weinberger, D.R. (1993). Three-dimensional surface rendering in MRI morphometry: A study of the planum temporale. *Journal of Computer Assisted Tomography, 17(4),* 529-535.

Lancaster, J.L. and Martinez, M.J. (2016). MANGO: Multi-image analysis GUI [open access software]. UT Health Science Center at San Antonio, TX.

Larsen, J. P., Høien, T., Lundberg, I., & Ødegaard, H. (1990). MRI evaluation of the size and symmetry of the planum temporale in adolescents with developmental dyslexia. *Brain and language, 39(2)*, 289-301.

Leonard, C.M., Voeller, K.K., Lombardino, L.J., Morris, M.K., Hynd, G.W., Alexander, G.W., Alexander, A.W., Andersen, H.G., Garofalakis, M., Honeyman, J.C., & Mao, J. (1993). Anomalous cerebral structure in dyslexia revealed with magnetic resonance imaging. *Arch Neurol., 50,* 461-469.

Le Troter, A., Auzias, G., & Coulon, O. (2012). Automatic sulcal line extraction on cortical surfaces using geodesic path density maps. NeuroImage, 61(4), 941-949.

Lombardo, M.V., Ashwin, E., Auyeung, B. Chakrabarti, B., Taylor, K., Hackett, G., Bullmore, E.T., & Baron-Cohen, Simon. Fetal testosterone influences sexually dimorphic gray

matter in the human brain. *Journal of Neuroscience, 32(2),* 674-680.

Marie, D., Jobard, G., Crivello, F., Perchey, G., Petit, L., Mellet, E., ... & Tzourio-Mazoyer, N. (2015). Descriptive anatomy of Heschl's gyri in 430 healthy volunteers, including 198 left-handers. *Brain Structure and Function*, *220*(2), 729-743.

McGuire, P.K., Silbersweig, D.A., & Frith, C.D. (1996) Functional neuroanatomy of verbal self-monitoring. *Brain 119*, 907–917

Musiek, F.E., Shinn, J.B., Jirsa, R., Bamiou, D.E., Baran, J.A. & Zaidan, E. (2005). GIN (gaps-in-noise) test in performance in subjects with confirmed auditory nervous system involvement. *Ear & Hear, 26(6),* 608-618.

Musiek, F.E. & Baran, J.A. (2007). The Auditory System: Anatomy, physiology and clinical correlates. Boston, MA: Pearson Education, Inc.

Naeser, M. A., Helm-Estabrooks, N., Haas, G., Auerbach, S., & Srinivasan, M. (1987). Relationship between lesion extent in'Wernicke's area'on computed tomographic scan and predicting recovery of comprehension in Wernicke's aphasia. *Archives of Neurology, 44(1)*, 73.

Nikkuni, S., Yashima, Y., Ishige, K., Suzuki, S., Ohno, E., Kumashior, H., Kobayashi, E., Awa, H., Mihara, T., & Asakura, T. (1981). Left-right hemispheric asymmetry of cortial speech zones in Japanese brains, *No to Shinkei, 33(1),* 77-84.

Obleser, J. & S.A. Kotz. 2009. Expectancy constraints in degraded speech modulate the language comprehension network. *Cereb. Cortex*. doi: 10.1093/cercor/bhp128.

Oertel-Knöchel, V., Knöchel, C., Matura, S., Prvulovic, D., Linden, D. E., & van de Ven, V. (2013). Reduced functional connectivity and asymmetry of the planum temporale in

patients with schizophrenia and first-degree relatives. *Schizophrenia research, 147(2),* 331-338.

Pah, G., Rankin, P., Cross, J.H., Croft, L., Northam, G.B.,…Baldeweg, T. (2013). Asymmetry of planum temporale constrains interhemispheric languageplasticity in children with focal epilepsy. *Brain, 136(1),* 3163-3175.

Papoutsi, M., de Zwart, J.A., Jansman, J.M, et al. (2009). From phonemes to articulartory codes: an fMRI study of the role of Broca's area in speech production. *Cereb Cortex, 19*, 2156-2165.

Price, C. J. (2010). The anatomy of language: a review of 100 fMRI studies published in 2009. Annals of the New York Academy of Sciences, 1191(1), 62-88.

Rademacher, J., Caviness Jr, V. S., Steinmetz, H., & Galaburda, A. M. (1993). Topographical variation of the human primary cortices: implications for neuroimaging, brain mapping, and neurobiology. *Cerebral Cortex*, *3*(4), 313-329.

Ratnanather, J. T., Poynton, C. B., Pisano, D. V., Crocker, B., Postell, E., Cebron, S., ... & Barta, P. E. (2013). Morphometry of superior temporal gyrus and planum temporale in schizophrenia and psychotic bipolar disorder. *Schizophrenia research, 150(2),* 476-483.

R Core Team (2019). R: A language and environment for statistical computing. R Foundation for Statistical Computing, Vienna, Austria. Retrieved from: https://www.R-project.org/.

Ruytjens, L., Georgiadis, J.R., Holstege, G., Wit, H.P., Albers, F.W.J, & Willemsen, A.T. (2007). Functional sex differences in human primary auditory cortex. *Nucl Med Mol Imaging, 34(12),* 2073-2081.

Ruytjens, L., Albers, F., van Dijk, P., Wit, H., Willemsen, A. (2007). Activation in primary

auditory cortex during silent lipreading is determined by sex. *Audiol Neurotol, 12,* 371-377.

Seldon, H.L. (1981). Structure of human auditory cortex. I. Cytoarchitectonics and dendritic distributions. *Brain Res, 229,* 277-291.

Shapleske, J., Rossell, S.L., Woodruff, P.W.R., & David, A.S. (1999). The planum temporale: A systematic, quantitative review of its structural, functional and clinical significance. *Brain Research Reviews, 29,* 26-49.

Smith, K.R., Hsieh, I.H., Saberi, K., & Hickock, G. (2009). Auditory spatial and object processing in the human planum temporale: No evidence for selctivity. *Journal of Cognitive Neuroscience, 22(4),* 632-639.

St. George, B., DeMarco, A.T., & Musiek, F. (2016, April 15). Revisiting anatomical variability along the Sylvian fissure: Its impact on central auditory research. 28th annual AudiologyNOW! Meeting, Phoenix, AZ.

Stein, J.L., Medland, S.E., Vasquez, A.A., Hibar, D.P., Senstad, R.E., Winkler, A.M. (2012). Identification of common variants associated with human hippocampal and intracranial volumes. *Nature Genetics, 44(5),* 552-561.

Steimetz, H., Rademacher, J., Huang, Y., Hefter, H., Zilles, K., Thron, A., & Freund, H. (1989). Cerebral asymmetry: MR planimetry of the human planum temporale. *Journal of Computer Assisted Tomography, 13(6),* 996-1005.

Steinmetz, H., & Galaburda, A. M. (1991). Planum temporale asymmetry: In-vivo morphometry affords a new perspective for neuro-behavioral research. In *Reading Disabilities* (pp. 143-155). Springer Netherlands.

St. George, B., DeMarco, A.T., & Musiek, F. (2017, April 13). Modern views on the anatomy of planum temporale. 29th annual AudiologyNOW! Meeting, Indianopolis, IN.

Teszner, D., Tzavaras, A., Gruner, J., & Hecaen, H. (1972). L'asymetrie droite-gauche du planum temporale; a propos de l'etude anatomique de 100 cerveaux. *Revue Neurologique, 126,* 444-449.

Thivard, L., Belin, P., Zilbovicius, M., Poline, J.B., & Samson, Y. (2000). A cortical region sensitive to auditory spectral motion, *Neuroreport,11(13),* 2969-72.

Tourville, J.A., Reilly, K.J., & Guenther, F.H. (2008). Neural mechanisms underlying auditory feedback control of speech. *NeuroImage, 39(3),* 1429-1433.

Tzourio-Mazoyer, N. & Mazoyer, B. (2017). Variation of planum temporale asymmetries with heschl's gyri duplications and association with cognitive abilities: MRI investigation of 428 health volunteers. *Brain Struct Funct, 222(6),* 2711-2726.

Vouloumanos, A., Kiehl, K.A., Werker, J.F. & Liddle, P.F (2001). Detection of sounds in the auditory stream: event-related fMRI evidence for differential activation to speech and nonspeeech. *J Cogn Neurosci, 13(7),* 994-1005.

Warren, J.D., Zielinski, B.A., Green, G.R., Rauschecker, J.P., & Griffiths, T.D. (2002). Perception of sound-source motion by the human brain. *Neuron, 34(1*), 139-148.

Wise, R., Chollet, F., Hardar, U., Riston, K., Hoffner, E., & Frackowiak, R. (1991). Distribution of cortical neuronal networks involved in word comprehension and word retrieval. *Brain , 114,* 1803-1817.

Witelson, S. F., & Kigar, D. L. (1992). Sylvian fissure morphology and asymmetry in men and women: bilateral differences in relation to handedness in men. Journal of Comparative

Neurology, 323(3), 326-340.

Wolpaw, J.R. & Penry, J.K. (1975). A temporal component of the auditory evoked response. *Electroencephalogr. Clin. Neurophysiol., 39,* 609-620.

Zach, P., Krištofiková, Z., Mrzílková, J., Majer, E.,…Kenney J. (2009). Planum temporale analysis via a new volumetric method in autoptic brains of demented and psychotic patients. *Current Alzheimer Research, 6(69).,* 69-76.

Zaehle, T., Wüstenberg, T., Meyer, M., & Jäncke, L. (2004). Evidence for rapid auditory perception as the foundation of speech processing : a sparse temporal sampling fMRI study. *European Journal of Neuroscience, 20,* 2447-2456.

Zatorre, R.J, Evans, A.C., Meyer, E., & Gjedde (1992). Lateralization of phonetic and pitch discrimination in speech processing. *Science, 256,* 846-849.

Zatorre, R.J., Bouffard, M., Ahad, P., & Bellin, P. (2002). Where is "where in the human auditory cortex? *Nature Neuroscience, 5,* 905-909.